

**UNCLASSIFIED**



**Australian Government**

**Department of Defence**  
Science and Technology

## Calculation of High Frequency Land Backscatter Coefficients

*Benjamin Slimming and Manuel Cervera*

**National Security, Intelligence, Surveillance and Reconnaissance Division**  
**Defence Science and Technology Group**

**DST-Group-TR-3613**

### **ABSTRACT**

A suitable model of the return ground clutter is required to help assess the performance of over-the-horizon radar. Currently, models for the clutter reflected from the sea exist but there are no models for the backscatter from land. The backscatter coefficient, which characterises the backscattered power, can be determined by considering the difference between observed backscatter ionograms and synthesised ionograms. The synthesised ionograms were generated using a MATLAB ray tracing toolbox, PHaRLAP, and the JORN Real Time Ionospheric Model. Data from the Laverton and Longreach backscatter sounders in September 2015 were analysed and backscatter coefficient results for sea, desert, plateau and hilly terrain in the Northern Territory were determined. It was found that the backscatter coefficient was large for hilly and rough terrains. Conversely, flat, dry deserts produced a lower backscatter coefficient.

### **RELEASE LIMITATION**

*Approved for public release*

**UNCLASSIFIED**

UNCLASSIFIED

*Produced by*

*National Security and Intelligence, Surveillance and Reconnaissance Division  
Third Avenue  
Edinburgh, SA 5111*

*Telephone: 1300 333 362*

*Copyright Commonwealth of Australia 2019  
June 2019*

**APPROVED FOR PUBLIC RELEASE**

UNCLASSIFIED

# Calculation of High-Frequency Land Backscatter Coefficients

## Executive Summary

To assess the performance of over-the-horizon radar, a reliable model of the return clutter is necessary. The ionosphere, the various propagation losses and backscatter from the sea are well understood; however, a suitable model for the return backscatter from land is lacking. This is due to the variable nature of the terrain.

Five regions in Northern Australia were analysed and a dataset for the land backscatter coefficients was collated. The data analysis involved comparing the difference between observed backscatter ionograms (plots of the return power as a function of group range and frequency) and synthesised ionograms. The synthesised ionograms were produced using a ray tracing toolbox, PHaRLAP, and the JORN Real Time Ionospheric Model. Range-frequency data cells that contained only one mode of propagation were considered. This was enforced by using filters and manually selecting the desired area on the observed ionogram.

For the purpose of validation of the methodology, sea backscatter was analysed. A sea backscatter coefficient of -22.5 dB was determined, which agrees well with theory for a fully developed sea state. The Simpson Desert was found to have a low backscatter coefficient of -35.0 dB and the Tanami Desert region in the Northern Territory had an aspect sensitive backscatter coefficient of -34.8 dB and -29.4 dB as measured by the Laverton and Longreach sounders respectively. A region in the north of NT near the Daly River had a large backscatter coefficient of -19.7 dB. This region has undulating terrain and we hypothesise that this is the cause of the relatively large value for the backscatter coefficient. The Longreach and Laverton sounders were also used to investigate a region in Central Arnhem in the north of NT. Values of -23.7 dB and -27.5 dB were determined as the backscatter coefficients for this region. We hypothesize that the larger value is due to aspect sensitive backscatter from the Mitchell Ranges in this region.

UNCLASSIFIED

*This page is intentionally blank.*

UNCLASSIFIED

## Authors

### **Benjamin Slimming**

University of Adelaide

Benjamin Slimming is studying a Bachelor of Mechanical Engineering and Bachelor of Science (majoring in theoretical physics) at the University of Adelaide. Over the 2018/19 summer break he was involved in the Summer Vacation Program (SVP) at DST Group.

---

### **Manuel Cervera**

National Security and Intelligence Surveillance and Reconnaissance Division

Manuel Cervera is a Discipline Lead (Propagation and Modelling) in the High Frequency Radar Branch of the National Security and Intelligence, Surveillance and Reconnaissance Division. He graduated with PhD in Meteor Physics in the Space and Atmospheric Physics group at the University of Adelaide in 1996. Since then he has worked continuously for DST Group. Principle interests are the propagation of HF radio waves through the ionosphere, ionospheric physics and the effects of ionospheric disturbances on HF radiowave equipment.

---

UNCLASSIFIED

*This page is intentionally blank.*

UNCLASSIFIED

## Contents

1. INTRODUCTION.....	1
2. THEORY .....	2
2.1. The Ionosphere and High Frequency Radar Propagation .....	2
2.2. Backscatter Ionograms .....	2
3. PROCESS.....	4
3.1. PHaRLAP.....	4
3.2. Real Time Ionospheric Model (RTIM) .....	5
3.3. Data Processing Method.....	6
4. RESULTS .....	8
4.1. Indian Ocean Backscatter Coefficient.....	8
4.2. Simpson and Tanami Desert Backscatter Coefficients.....	9
4.3. Daly River and Central Arnhem, NT Backscatter Coefficients .....	11
4.4. Elevation and frequency dependence.....	13
5. DISCUSSION .....	15
6. CONCLUSION .....	16
7. ACKNOWLEDGEMENTS .....	16
8. REFERENCES .....	17
APPENDIX A BACKSCATTER COEFFICIENT MATLAB CODE	
DESCRIPTION .....	19
A.1. RTIM and BSS Observation Temporal Matching.....	19
A.2. Synthetic Backscatter Ionogram Generation .....	19
A.3. Manual Data Processing and Determination of Backscatter Coefficient	
Values .....	19
A.4. Viewing Results from the Backscatter Coefficient Data.....	20
A.5. Automation of Data Processing.....	20

UNCLASSIFIED

DST-Group-TR-3613

*This page is intentionally blank.*

UNCLASSIFIED

# 1. Introduction

This study has developed an understanding of the land backscatter coefficients at various locations around Australia by using the Jindalee Over-The-Horizon Radar Network (JORN) backscatter sounders. Over-the-horizon radar (OTHR) uses the ionosphere to detect targets beyond the horizon up to 3000 km away. Transmitted high frequency (HF) radio waves either penetrate the ionosphere or are refracted down towards the Earth's surface. Of the rays that hit the Earth's surface, some of the power will be scattered back towards the receiver and appear as undesirable (i.e. non-target) echoes called clutter. The amount of clutter power depends upon the propagation losses through the ionosphere and the ground backscatter coefficient.

To assess the performance of OTHR, a reliable model of the returned clutter is necessary. The High Frequency Radar Branch at DST has a sound knowledge of signal losses in the ray propagation. However, the branch does not have a suitable model of the clutter that is reflected by land.

While much work has been conducted on sea backscatter by various researches (e.g. Munk and Nierenberg (1969) and Barrick (1972)), research into land backscatter coefficients has been limited. Li (1998) generated a formula for a land backscatter coefficient in China as a function of elevation. However, the statistical sample size was small and only 200 data points were used. Furthermore, a methodology was not specified and when Li validated the data the source was not provided.

In this study, the backscatter coefficients have been determined by comparing observed backscatter ionograms with synthesised ionograms generated in MATLAB (Mathworks, 2018). The synthesised ionograms have been developed using PHaRLAP (Cervera & Harris, 2014), and were based on the numerical ray tracing (NRT) algorithms developed by Coleman (1998). Data from the Laverton East and Longreach backscatter sounders were used to determine backscatter coefficients for several regions: sea, desert, and plateau and hilly terrain in the Northern Territory.

This report details the process for collecting and simulating the data used to calculate the backscatter coefficient. In Section 2, the theory behind the ionosphere and backscatter ionograms is presented. Section 3, details the process of the method and simulation of the synthesised ionograms. Results are presented in Section 4 and a discussion of future work is found in Section 5.

## 2. Theory

### 2.1. The Ionosphere and High Frequency Radar Propagation

Ultra-violet radiation from the sun ionises molecules in the air at heights from 60 km to over 1000 km (Davies, 1990; McNamara, 1991). Within this region, four layers are present. In order of increasing altitude the D, E, F1 and F2 layers complete what is known as the ionosphere. Using the ionosphere, high frequency radio waves can be refracted down to ground, provided that the frequency is not so large enough that they penetrate. The propagating radio waves may return to ground in a number of ways. F-high, F-low and E modes may contribute to the propagation of power to a particular patch of ground and Figure 1 shows an example of these propagation modes. During the propagation of the ray, energy will be absorbed, which occurs mainly in the D region. Furthermore, multi-hop modes are possible. This occurs when the ray from the ground forward scatters into the ionosphere and refracts back to Earth again.

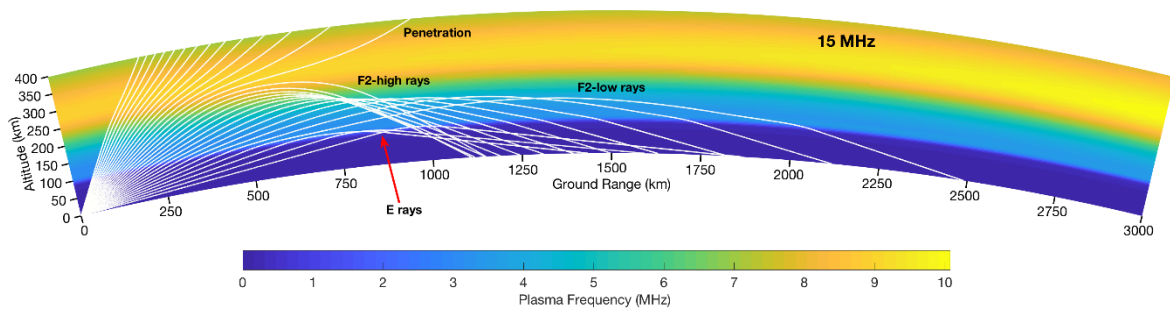


Figure 1. Radar rays may penetrate the ionosphere or be refracted from the F or E layers back to Earth

### 2.2. Backscatter Ionograms

A backscatter sounder is an environmental radar that may be used to determine the best frequency for observing a particular range. The JORN frequency management system (FMS) (Earl & Ward, 1987) employs backscatter soundings of the ionosphere for this purpose. Backscatter ionograms are generated from the sounders. These backscatter ionograms are plots of the returned power as a function of frequency and group range. The received power,  $P_R$ , is given by the Radar Equation:

$$P_R = \frac{\lambda^2 \sigma_0 \Delta A P_T}{(4\pi)^3 d_T^2 d_R^2} G_T G_R L_T L_R$$

where  $P_T$  is the transmitted power,  $\lambda$  is the signal wavelength,  $\Delta A$  is the area of the flux tube intersecting the Earth,  $d_T$  and  $d_R$  are effective distances along the transmitted and received paths respectively,  $G_T$  and  $G_R$  are transmit and receive gains respectively and  $L_T$  and  $L_R$  are the absorption losses for the transmitted and received paths.  $\sigma_0$  is the

backscatter coefficient. The effective distance accounts for focussing and defocussing of the radio waves and is given by (Davies, 1990; Coleman, 1997):

$$d = \left( \frac{R_e \sin\left(\frac{D}{R_e}\right) \sin(\beta_F) \Delta D}{\cos(\beta_i) \Delta\beta_i} \right)^{0.5}$$

This formula applies for pairs of rays launched at elevations of  $\beta_i$  and  $\beta_i + \Delta\beta$ .  $R_e$  is the radius of the Earth,  $D$  is the ground range,  $\Delta D$  is the length of the ground range covered by the flux tube and  $\beta_F$  is the elevation of the ray at the landing point.

During this study, backscatter ionograms were used to determine backscatter coefficients by accounting for all the other propagation losses. An example backscatter ionogram is shown in Figure 2. Annotated on this ionogram is the leading edge, the locus of minimum group range for which power is received as a function of frequency (McNamara, 1991). Other annotated features such as sporadic-E and meteors are beyond the scope of this report and are not discussed further. However, see standard texts (e.g. Davies, 1990) for details.

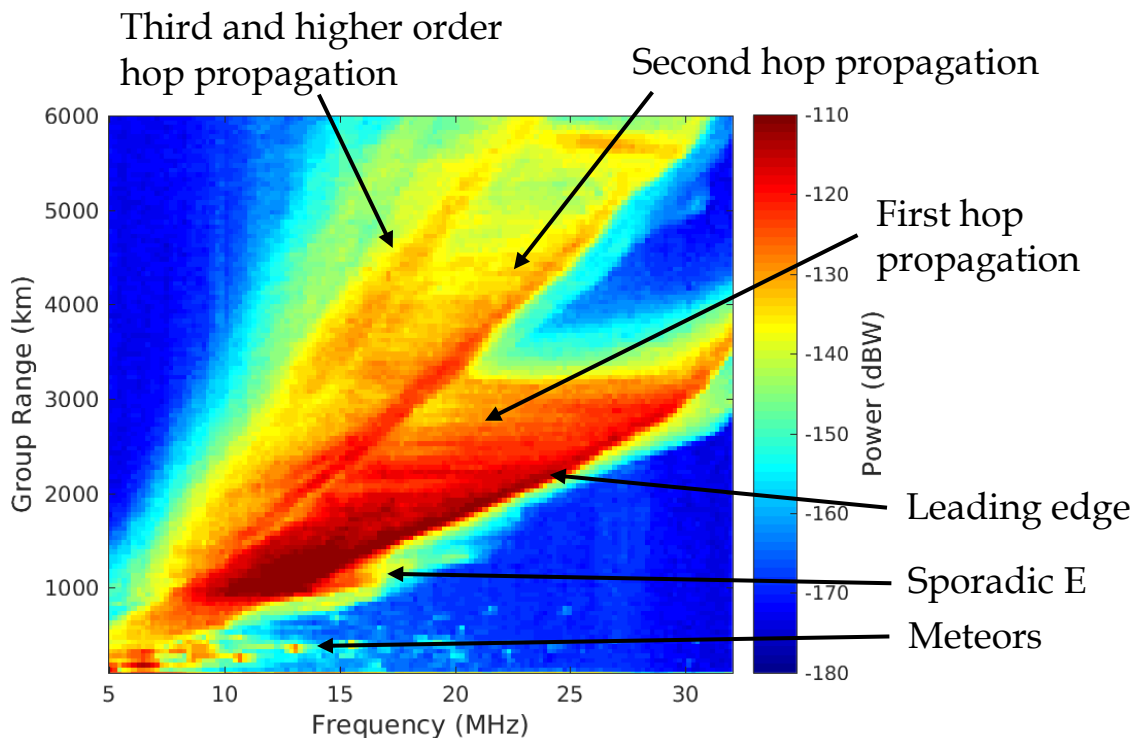


Figure 2. An annotated backscatter ionogram displaying multiple hop propagation

### 3. Process

Land backscatter coefficients were found by considering the difference between the observed ionogram and a synthesised ionogram. The synthesised ionogram was created using PHaRLAP ray tracing algorithms and the Real Time Ionospheric Model (RTIM).

#### 3.1. PHaRLAP

PHaRLAP (Provision of High-frequency Raytracing Laboratory for Propagation studies) is a MATLAB ray tracing toolbox (Cervera & Harris, 2014) that models the propagation of a fan of high frequency radio waves through the ionosphere. This toolbox uses the ray propagation results at different frequencies and elevations to develop a synthesised backscatter ionogram.

Within PHaRLAP, a 3D ray tracing engine is available that considers effects of the Earth's magnetic field and ionospheric out of plane gradients on the ray propagation. Coleman (1997) suggests that 2D ray tracing is suitably accurate and the simulation speed is much faster. 2D numerical ray tracing (NRT) with PHaRLAP has been used in previous studies (Cervera et al., 2018). Therefore, 2D ray tracing was used for the generation of the synthesised backscatter ionograms.

The received power,  $P_R$ , modelled by PHaRLAP is given by the Radar Equation discussed in Section 2.2. The flux tube area,  $\Delta A$ , can be determined using an adaptation of what was used by Coleman (1997):

$$\Delta A = R_e \sin\left(\frac{D}{R_e}\right) \left(\frac{dD}{d\beta}\right) \Delta\beta \Delta\phi$$

where  $R_e$  is the radius of Earth,  $D$  is the ground range of the ray,  $\beta$  is the transmitted elevation angle,  $\Delta\beta$  is the elevation step of the fan of rays and  $\Delta\phi$  is the azimuthal beam width.

Within this analysis, the backscatter coefficient,  $\sigma_0$  was neglected (i.e. set to 0 dB) for the production of the synthesised backscatter ionograms. This enabled the backscatter coefficient to be determined by considering the difference between the observed backscatter ionograms and the synthesised ionograms for each valid individual range-frequency cell. Valid range-frequency cells are those where only one propagation mode contributes power. The process for determining these cells is described in Section 3.3.

Within PHaRLAP, rays launched at different elevations are traced through the ionosphere. As the rays propagate, the losses are accounted for and the power is evenly distributed through the modelled flux tube. The antenna gains,  $G_T$  and  $G_R$ , were based on the antenna pattern of the corresponding sounder.

Absorption in the ionosphere was found by using the model generated by George and Bradley (1974). In addition, a polarisation mismatch loss of 3 dB on reception was included

within the synthesised model. Figure 3 displays an example of a synthesised backscatter ionogram using a notional land backscatter coefficient of -26 dB.

### 3.2. Real Time Ionospheric Model (RTIM)

The Australian Defence Force operates a number of oblique and vertical incidence sounders around Australia which constantly monitor the ionosphere. The purpose of these sounders is to generate a near real time model of the ionosphere required to accurately register targets observed by JORN (Cameron, 1995). We do not comment further on the RTIM other than to note that this model of the ionosphere is used for the ray tracing analysis required for synthesising the model backscatter ionograms. Monthly median climatological models, such as the International Reference Ionosphere (IRI), could be used but they do not model the day-to-day variability of the ionosphere and so will not provide an accurate representation of the ionosphere at the time of interest.

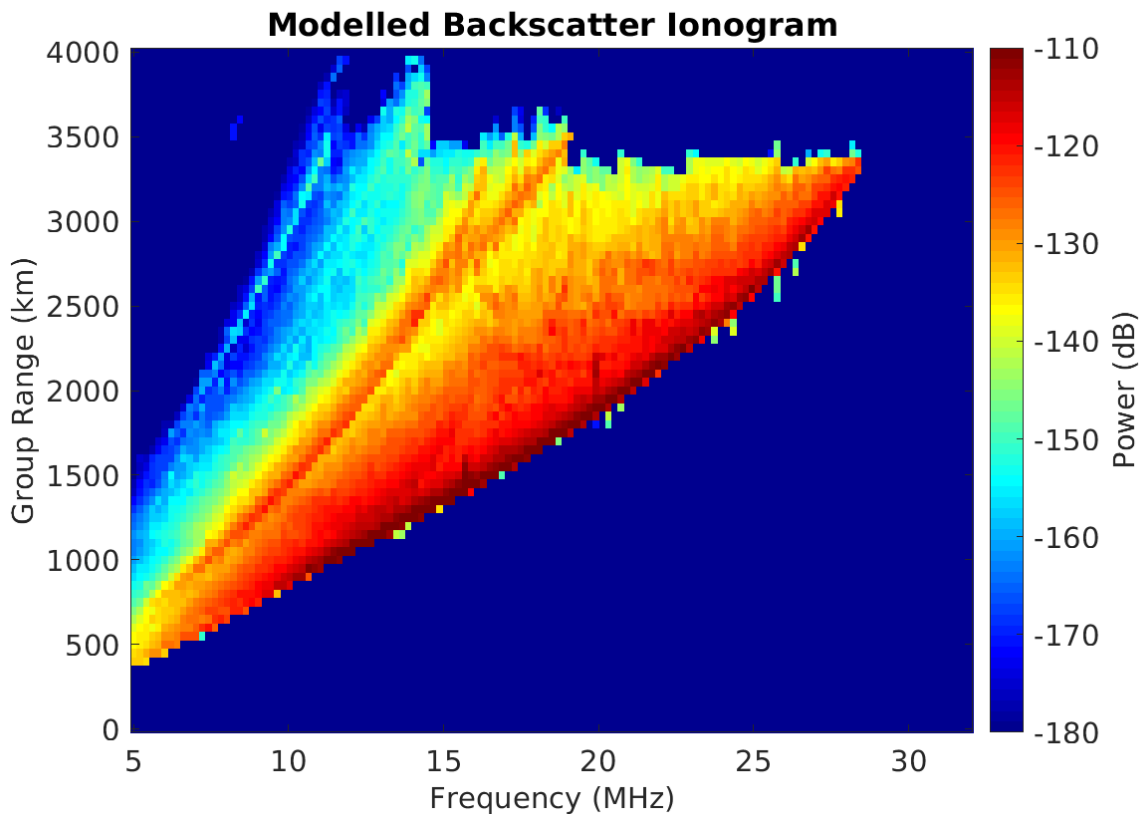


Figure 3 Example of a synthesised ionogram generated using PHaRLAP for 27 September 2015 at 7:15:00 UTC (15:15 Australian Western Standard Time). The sounder location was Laverton, WA and the bearing was 29 degrees from true North (Laverton East FMS beam 4).

### 3.3. Data Processing Method

For each observed ionogram, a co-temporal ionosphere from the RTIM was imported into PHaRLAP and a model backscatter ionogram was generated. The ionospheric model data provided from the RTIM was spatially limited as it extended only to 1600 km from the backscatter sounder. This required care when modelling the ionograms.

Data was taken for the days listed in Table 1. As the ionosphere appeared to be most geomagnetically stable from 24 to 30 September (Neudegg, 2018), the initial dataset was taken from this period. However, data from the Longreach backscatter sounder was limited during this time. Therefore, additional data was taken from the week earlier. The ionosphere is stronger during the day, yielding clearer ionograms. Hence, a condition was applied to only include data between 0:00 and 10:00 UTC. This is approximately 9:00 – 19:00 Local Solar Time.

Table 1. Data was collected from Laverton East and Longreach in late September 2015

Backscatter Sounder	Beam	Start Date	End Date
Laverton East	1	23/09/2015	28/09/2015
Laverton East	4	18/09/2015	28/09/2015
Laverton East	5	18/09/2015	28/09/2015
Laverton East	8	23/09/2015	28/09/2015
Longreach	1	18/09/2015	22/09/2015
Longreach	4	18/09/2015	22/09/2015

It is important to use data from the ionogram which has only one significant mode contributing to the range-frequency cell. Different modes of propagation will have different elevations and the backscatter coefficient is expected to be elevation dependent. To isolate a single backscatter coefficient, range-frequency cells with one mode of propagation is needed. For each ionogram, a region was selected which corresponded to one-hop propagation only and was away from the leading edge. Staying away from the leading edge is necessary to reduce focusing effects and to avoid F2-high rays. Shown in Figure 4 is an example of the selected area. Automatically selecting a region for the first hop corresponding to the F2-low rays on an observed ionogram is difficult, therefore a region was manually selected on each ionogram.

Filters were applied to the selected cells to ensure that only one significant mode of propagation contributes to the ionogram. These filters are explained in Table 2.

While the PHaRLAP ray tracing engine is accurate it is only as good as the input ionospheric electron density grid. The specification of the electron density grid is the major source of error in determining where the energy (i.e. the rays) propagates to the ground. The other major source of error is the George and Bradley ionospheric absorption model. Errors in this model will contribute to the errors in the estimation of the amount of energy that propagates to a particular patch of ground.

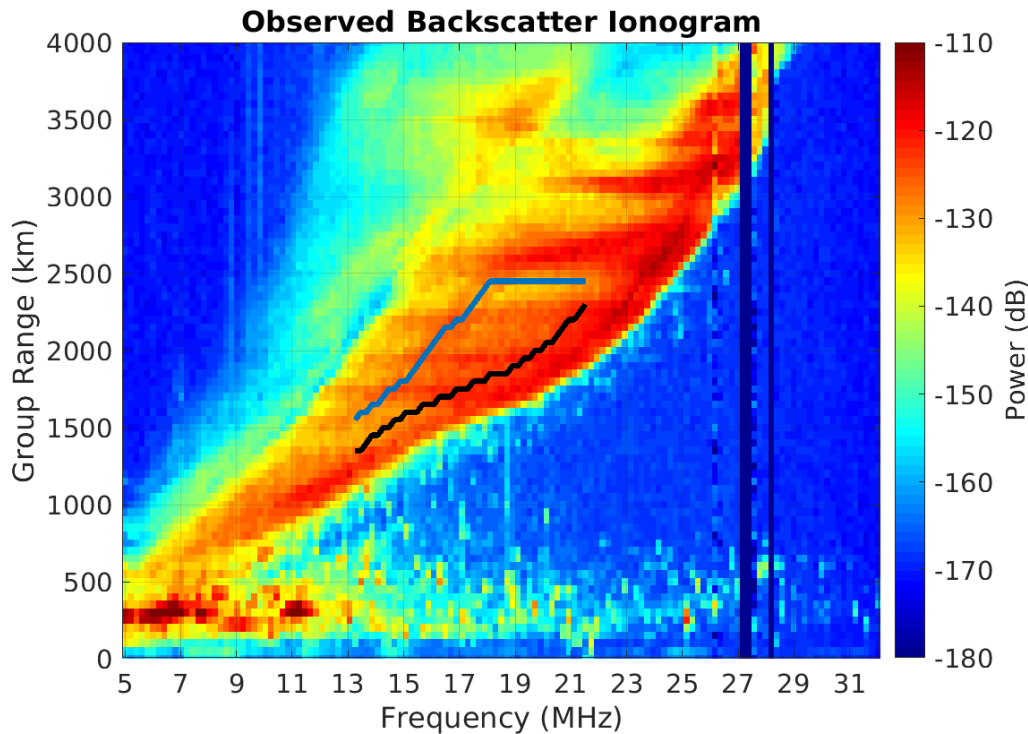


Figure 4. Example showing selection of region from the observed ionograms. The selected cells were further filtered and analysed and a backscatter coefficient was found for each cell.

Table 2. Filters used to ensure that cells with only one mode of propagation were included for further analysis

Characteristic	Removal Method	Reason
Large ground ranges	Flag cells with rays that had a ray height above 80 km at a ground range of 1600 km.	The RTIM provided ended at 1600 km. Rays beyond this range at an altitude where refraction still occurs will not be accurate, yielding incorrect results.
E layer propagation mode	Flag cells with a ray apogee height of less than 150 km	If the power contributed from E layer propagation and High F propagation was less than the total power by less than 10 dB, then the cell was removed from the analysis. It is necessary to ensure that only F2 Low propagation modes are in the analysis.
F2 high propagation mode	Flag cells with $\frac{dD}{d\beta}$ greater than zero, where $D$ is the ground range and $\beta$ is the elevation of the ray.	

## 4. Results

Backscatter coefficients from five regions were calculated using the data from the sounder beams displayed in Figure 5. Each region investigated had a range depth of 200km. Backscatter from two of these regions in the Northern Territory were evaluated at different aspect angles with beams from Laverton and Longreach. A diagrammatic representation of the areas considered is shown in Figure 5 and the results from these regions are displayed in this section.

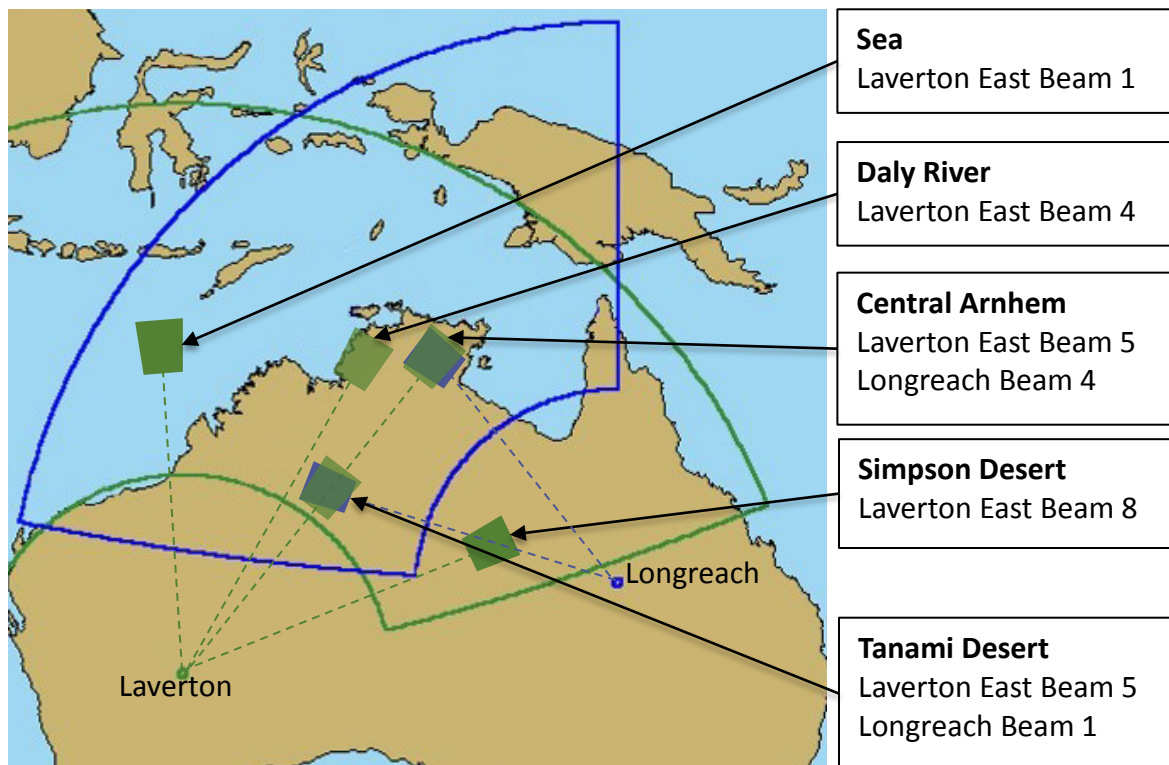


Figure 5 Map showing the five regions analysed by the Laverton and Longreach sounders. Two areas were analysed at different aspects. The range depth for each region is 200 km.

### 4.1. Indian Ocean Backscatter Coefficient

For validation of the methodology, Laverton East Beam 1 was used to calculate the backscatter coefficient of the sea. As shown in Figure 6, a median value of -22.5 dB was determined as the sea backscatter coefficient. This value is in close agreement with the accepted value of -23 dB for a fully developed sea (Munk & Nierenberg, 1969). The distribution of the backscatter coefficient has a large variance which is probably due to the variability of the ionosphere. We use the interquartile range as a measure of the spread in the backscatter coefficient which is 8.6 dB in this case. While the spread in values is large, we have confidence in the methodology due to the good agreement of the median with the accepted value and so apply it to land.

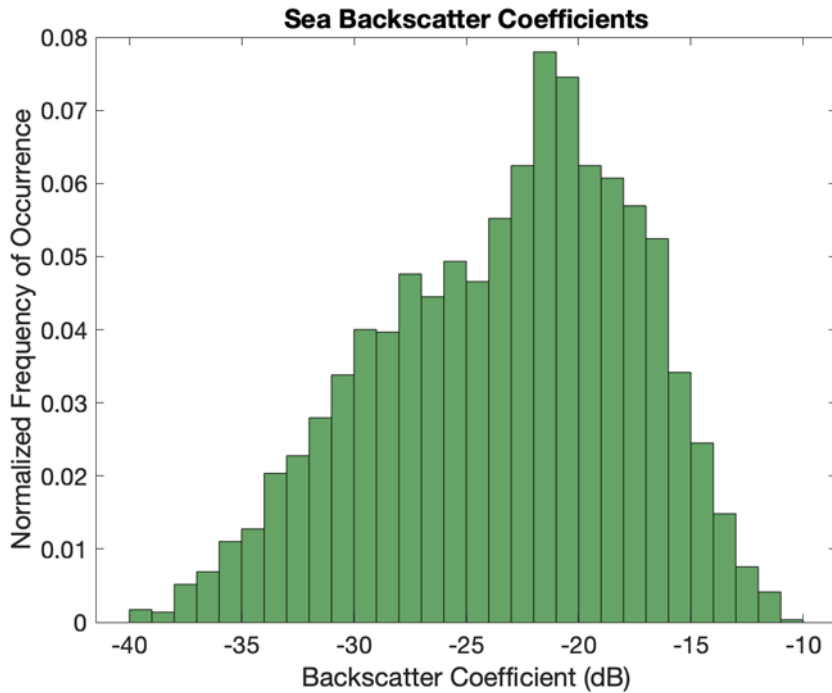


Figure 6. Histogram of measured sea backscatter coefficients using the Laverton East sounder. The median value for the sea backscatter coefficient was -22.5 dB and interquartile range 8.6 dB.

## 4.2. Simpson and Tanami Desert Backscatter Coefficients

Backscatter coefficients were determined for the Simpson and Tanami Deserts. The Simpson Desert results, displayed in Figure 7, has a median value of -35.0 dB with an interquartile range of 5.3 dB. The Tanami Desert results, displayed in Figure 8, had a median values for the backscatter coefficient of -34.8 dB and -29.4 dB as determined from the Longreach and Laverton sounders respectively. The interquartile ranges are 4.7 dB and 4.9 dB. The backscatter coefficient for desert is much lower than that of the sea (up to 12 dB lower) and this expected due to the dry, flat terrain.

It is interesting to note the aspect sensitivity of the backscatter coefficient of the Tanami Desert. We currently do not understand the cause of this but we speculate that it due to the nature of the terrain; elongated topographical features (e.g. hills / ridges) perpendicular to the direction to Longreach could cause enhanced backscatter in that direction. However, cursory inspection of the terrain using Google Maps does not reveal any such features. We also note that the variance of the data is less than that for the sea displayed in Figure 6. This is probably due to the static land as opposed to the variable nature of the sea state over the observation period.

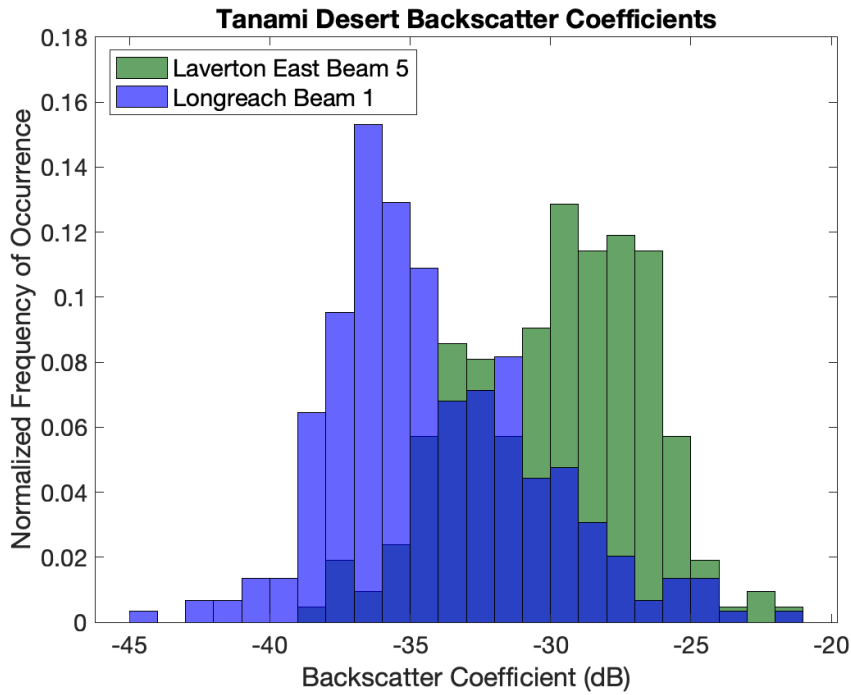


Figure 7. Histogram of measured backscatter coefficients for the Tanami Desert using the Laverton East and Longreach sounders. The median values were -29.4 dB and -34.8 dB with interquartile ranges of 4.9 dB and 4.7 dB respectively.

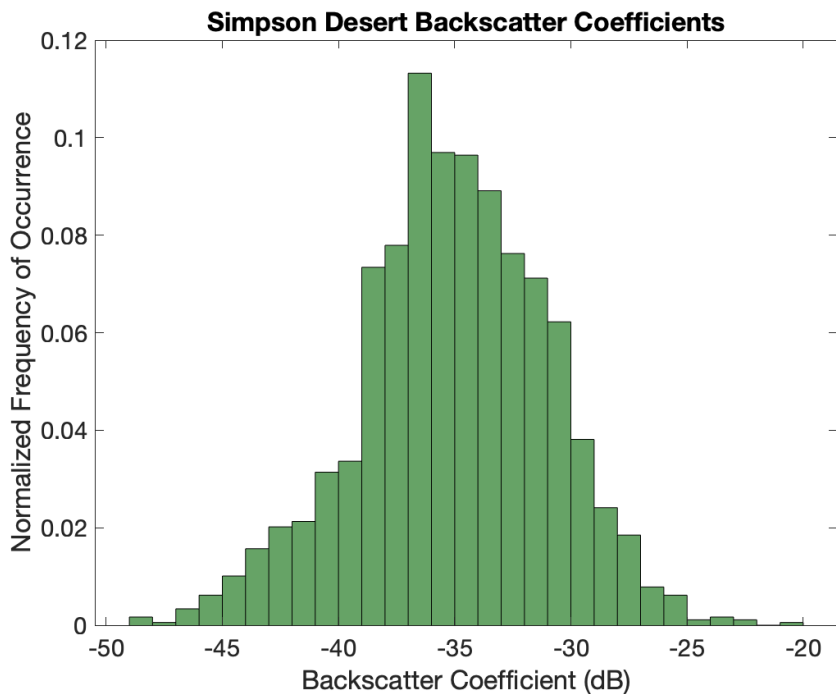


Figure 8. Histogram of Backscatter coefficients for the Simpson Desert. The median value is -35.0 dB and the interquartile range 5.3 dB.

### 4.3. Daly River and Central Arnhem, NT Backscatter Coefficients

The top end of the Northern Territory was examined in two separate regions: the area bounded by the Daly and Victoria rivers and the Central Arnhem area (see Figure 5). These two regions have different topography with the Daly river region having hilly undulating terrain. This is displayed in the topographic map in Figure 10. The Central Arnhem region was investigated using both the Laverton and Longreach sounders so any aspect sensitivity of the backscatter coefficient could be examined.

The Daly River region has a backscatter coefficient of -19.7 dB as measured by the Laverton Sounder (see Figure 9) with an interquartile range of 6 dB. The large backscatter coefficient was unexpected and it shows that this region of land scatters more energy than the sea. This is most likely due to the undulating and hilly terrain, which is prevalent throughout the entire region. The interquartile range is, as for the desert region examined in the previous section, less than that for sea which is expected.

The Central Arnhem region had an aspect sensitive backscatter coefficient which was lower than for the Daly river region. The Laverton and Longreach sounder data returned backscatter coefficients of -27.5 dB and -23.7 dB with interquartile ranges of 4.9 dB and 4.6 dB respectively. The high backscatter coefficient as measured by the Longreach sounder indicates that there are topographical features in this region which are aligned perpendicularly to the direction of the Longreach sounder beam 4. The Mitchell Ranges are the likely cause for the enhanced backscatter in the direction of Longreach.

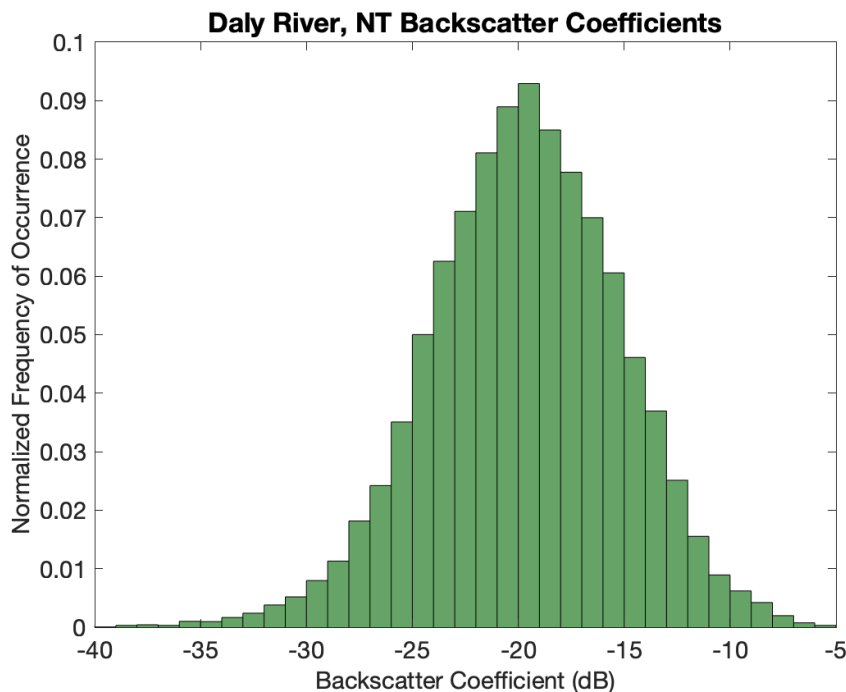


Figure 9. Histogram of measured backscatter coefficients near the Daly River, NT using the Laverton Sounder. The median value is -19.7 dB with an interquartile range of 6.0 dB.

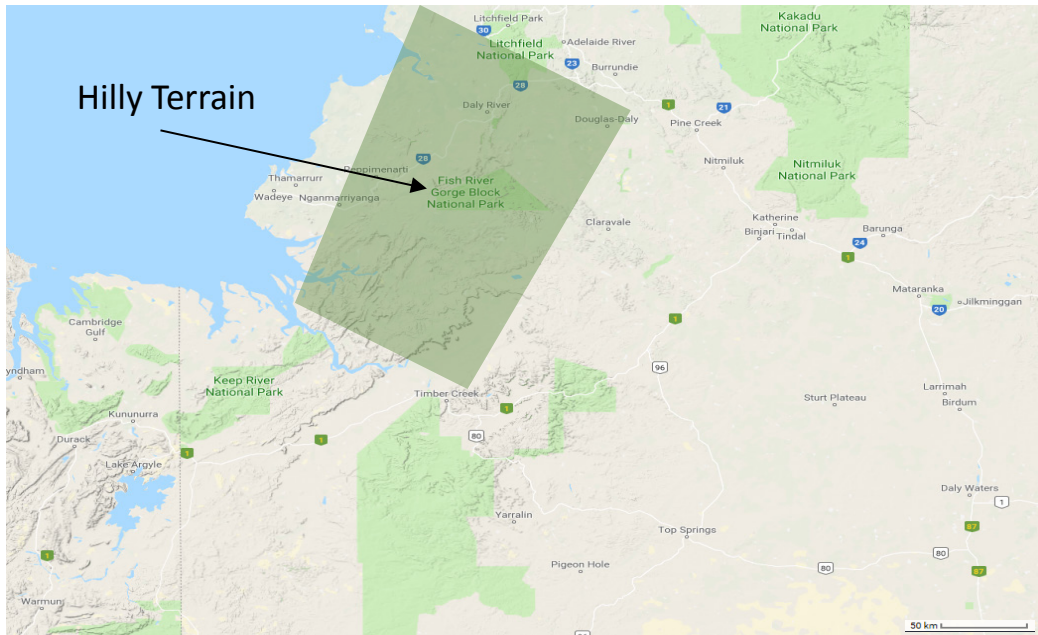


Figure 10. Map showing the hilly, undulating terrain in the Northern Territory between the Daly and Victoria Rivers (Google Maps, 2019).

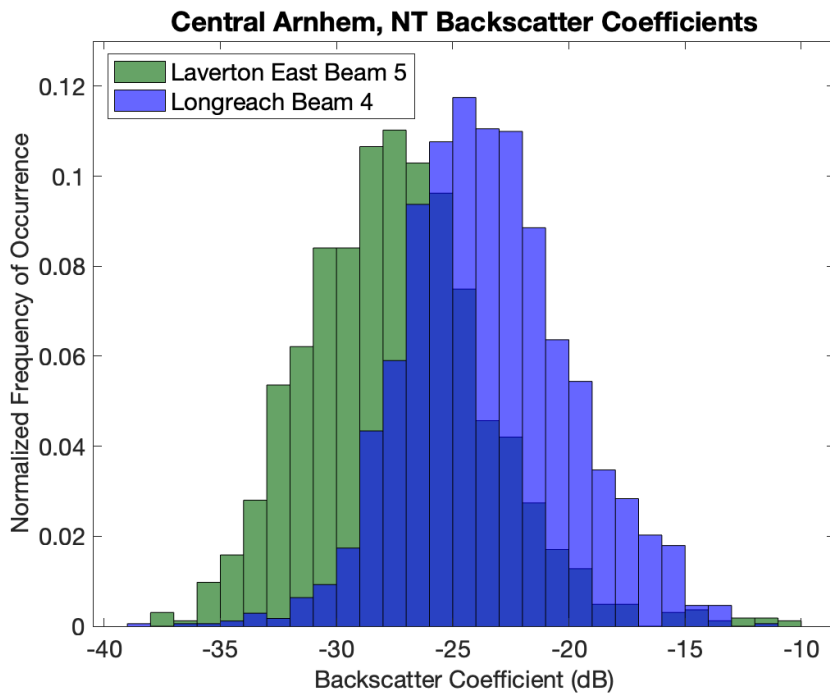


Figure 11. Histogram of measured backscatter coefficients for Central Arnhem using the Laverton East and Longreach sounders. The median values were -27.5 dB and -23.7 dB with interquartile ranges of 4.9 dB and 4.6 dB respectively.

#### 4.4. Elevation and frequency dependence

We attempted to determine the elevation dependence of the backscatter coefficient. The elevation was estimated from the launch angle of rays used to synthesise the model ionogram. Figure 12 displays the backscatter coefficient as a function of elevation for the Sturt Plateau derived from the Laverton BSS data. This region was selected as it had the most data from the flat terrain. As there is not a large range of elevations (between 12 and 18 degrees) and there is a large variation in the data, a clear trend could not be seen. Due to the limited range of elevations in general for OTHR propagation, we do not expect that this methodology would be successful in measuring the elevation dependence of the backscatter. Never-the-less a statistical analysis of the data was completed to attempt to find a functional form of the backscatter coefficient parameterised by frequency and elevation.

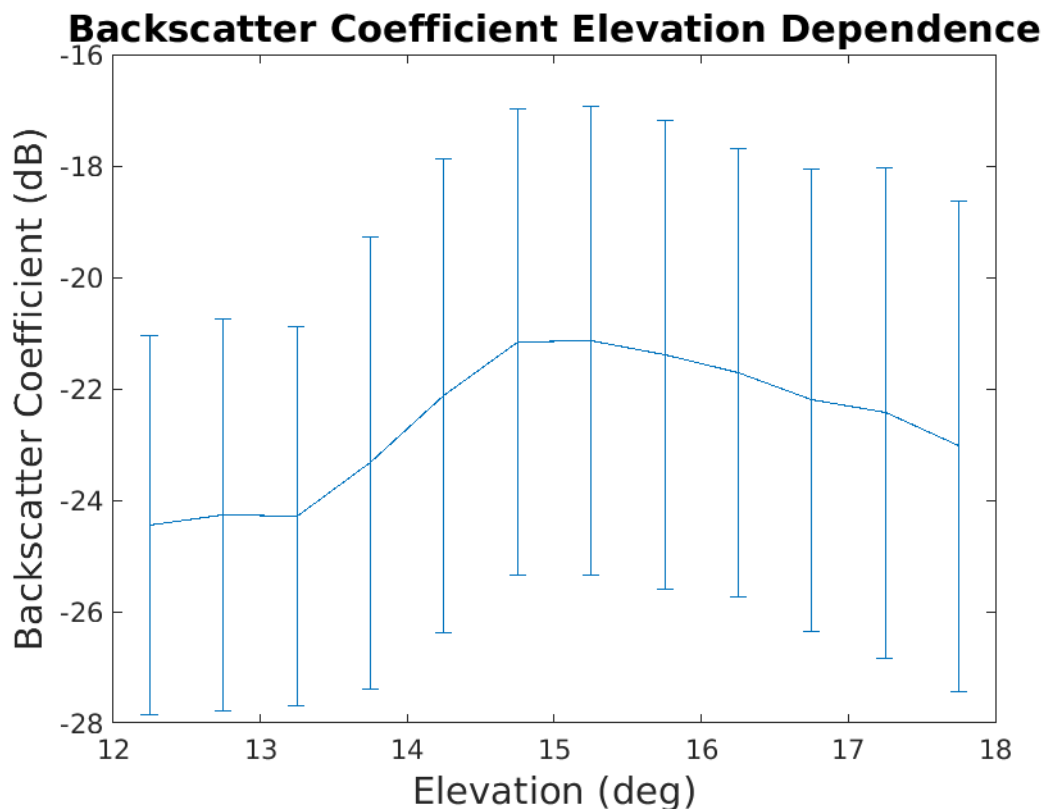


Figure 12. Measured backscatter coefficients as a function of elevation. The error bars are standard deviation. Data are from ground ranges of 1400 - 1800 km and frequencies between 14 and 16 MHz.

A Kolmogorov-Smirnov test was conducted to determine the normality of the data (Massey, 1951). Data from all beams with ground ranges of 1400 - 1800 km were included. The null hypothesis was that the backscatter coefficients followed a normal distribution with a mean and standard deviation equal to that of the dataset.

Table 3 shows the results of this test and most beams had the null hypothesis rejected with a 95% significance. As a result, simple statistical analysis techniques cannot be applied and a different procedure must be used to analyse the data. The functional dependence of the backscatter coefficient needs to be determined individually for each patch of ground that was examined.

Table 3. *Kolmogorov-Smirnov test for testing the normality of the backscatter coefficients from different beams. The null hypothesis was that the backscatter coefficients followed a normal distribution.*

Sounder	p value	Rejection of null hypothesis at 95% significance
Laverton East Beam 3	0.0023	Reject
Laverton East Beam 4	1.5e-5	Reject
Laverton East Beam 7	0.09	Fail to Reject
Longreach Beam 0	4.0e-5	Reject
Longreach Beam 3	0.02	Reject

A multiple variable regression analysis was performed to determine if there was a functional dependence,  $g$ , between the backscatter coefficient of Laverton East beam 4 in the ground ranges between 1550 and 1600 km and the frequency and elevation:

$$\sigma_0 = g(f, \beta)$$

where  $f$  is the ray frequency and  $\beta$  is the elevation launch angle.

A functional form was assumed as follows:

$$\sigma_0 = b_1 \sin(\beta) + b_2 f^4 + b_3 f^3 + b_4 f^2 + b_5 f + b_6 \sin(\beta) f^4 + b_7 \sin(\beta) f^3 + b_8 \sin(\beta) f^2 + b_9 \sin(\beta) f + b_{10}$$

The sine of the elevation dependence was chosen as with Li (1998). From canonical correlation analysis, the higher order frequency terms were not significant and could be removed from the analysis (Seber, 1984). Therefore, a regression was performed with a selected form of:

$$\sigma_0 = b_1 \sin(\beta) + b_4 f^2 + b_5 f + b_8 \sin(\beta) f^2 + b_9 \sin(\beta) f + b_{10}$$

The  $r^2$  statistic from the regression analysis had a value of 0.2833 which indicates the accuracy of the regression was poor. As such, it was impossible to determine a functional form of the backscatter coefficient. This result is probably due to the limited range of elevations and frequencies over which the backscatter coefficient was able to be calculated. As the elevations that are used to observe a particular patch of ground is determined by

the experimental geometry and state of the ionosphere it is unlikely that a greater range of elevations would be available. Thus, the only way for this sort of regression analysis to be successful is to reduce the variance in the measured backscatter coefficient, which in turn would require better models of the ionosphere and absorption.

## 5. Discussion

As seen in the figures from Section 4, the land backscatter coefficient is highly dependent on the terrain of the land. There was more backscatter in some areas of the Northern Territory than expected, due to the hilly terrain. Conversely, flatter regions that were analysed in the desert yielded smaller backscatter values. Further research would have to be undertaken with a larger data set to improve the model of the backscatter coefficient.

Currently, only 2D NRT is used for the generation of the synthesised backscatter ionograms. Computationally, this is less expensive than using 3D NRT. However, 3D NRT is able to account for various effects such as out of plane propagation due to the geomagnetic field and cross-range ionospheric gradients. Further, we note that the azimuth steer angle,  $\phi_{steer}$ , required to receive signals from an azimuth of,  $\phi_{target}$ , is functionally dependent on the elevation angle,  $\beta$ , as follows:  $\sin(\phi_{steer}) = \sin(\phi_{target}) \cos(\beta)$ . This effect, colloquially known as “coning” or “cone effect” is due to the linear receive arrays used by the sounders having a surface of constant phase in the shape of the cone. Coning was not modelled by the 2D NRT. The use of 3D ray tracing would account for this effect.

It is possible to receive backscatter sounder transmissions with the JORN main receive array (colloquially known as common aperture). This allows backscatter ionograms to be formed with a much finer azimuthal resolution. Currently, the azimuthal width for the areas considered in this report is very large. With a highly resolved azimuthal angle, the backscatter ionograms would be better resolved azimuthally and more accurate results can be achieved. The areas of interest, shown in Figure 5, would be finer and would produce less variable data.

Other factors which may be considered are frequency, time of day and soil moisture content. In the data that has been examined here, there aren't enough data points to isolate a particular variable. The variance in the data also makes it challenging to determine which variables influence the land backscatter coefficient. By considering more days with more azimuthally resolved data, it may become clearer what affects the backscatter coefficient.

## 6. Conclusion

From the analysis, it can be seen that backscatter ionograms may be used to determine ground backscatter coefficients. Synthesised backscatter ionograms were developed using numerical ray tracing tools and ionospheres from JORN's RTIM. Land backscatter coefficients were determined by comparing the observed ionograms to the synthesised ionograms. Data was taken from the Laverton East and Longreach backscatter sounders. Care was taken to ensure that data cells with only one mode of propagation were considered.

Five regions were analysed. The region in the Indian Ocean produced a median sea backscatter coefficient of -22.5 dB, which agrees with previous research for a fully developed sea. Desert regions were observed; the Simpson Desert had a median land backscatter coefficient of -35.0 dB and the Tanami Desert had median backscatter coefficients of -29.4 dB and -34.8 dB as measured from two different aspect angles. A hilly Northern Territory region produced a higher than expected land backscatter coefficient of -19.7 dB. Finally the Central Arnhem region in the Northern Territory had median backscatter coefficients of -27.5 dB and -23.7 dB when measured at two different aspect angles. The higher value could be due to the Mitchell Ranges. Clearly the topography of the terrain has a large impact on the backscatter coefficient.

Further research could be conducted to investigate other factor that influence the backscatter coefficient. Having a highly resolved azimuthal angle by using common aperture and using 3D ray tracing would improve the quality of results. More data would need to be collected to understand the full extent other factors such as soil salinity, moisture and frequency would have on the land backscatter coefficient.

## 7. Acknowledgements

We would like to thank David Francis, David Holdsworth, David Netherway, David Neudegg for their support and advice throughout the summer project. We also would like to thank Chris Crouch for providing the sounder and real time ionospheric model data.

## 8. References

- Barrick, D. E., (1972). First-Order Theory and Analysis of MF/HF/VHF Scatter from the Sea. *IEEE Transactions on Antennas and Propagation*, Vol. 20, pp. 1-10
- Cameron, A. (1995), The Jindalee Operational Radar Network: Its architecture and surveillance capability, in *Proceedings of the IEEE International Radar Conference*, pp. 692-697.
- Cervera, M. A., Francis, D. B., & Frazer, G. J. (2018). Climatological model of over-the-horizon radar. *Radio Science*, 53. doi:10.1029/2018RS006607
- Cervera, M. A., and T. J. Harris (2014), Modeling ionospheric disturbance features in quasi-vertically incident ionograms using 3-D magnetoionic ray tracing and atmospheric gravity waves, *J. Geophys. Res. Space Physics*, 119, 431-440, doi:10.1002/2013JA019247.
- Coleman, C. J., (1997) On the simulation of backscatter ionograms. *Journal of Atmospheric and Solar-Terrestrial Physics*, Vol. 59, pp. 2089-2099
- Coleman, C. J., (1998) A ray tracing formulation and its application to some problems in over-the-horizon radar, *Radio Science*, Vol. 33, pp. 1187-1997
- Davies, K. (1990) *Ionospheric Radio*, Peter Peregrinus Ltd, IET, London
- Earl, G. F., & Ward, B. D. (1987). The frequency management system of the Jindalee over-the-horizon backscatter HF radar. *Radio Science*, Vol. 22, pp. 275-291.
- George, P. L., & Bradley, P. A. (1974). A new method of predicting the ionospheric absorption of high frequency waves at oblique incidence. *Telecommunication Journal*, 41, 307-311.
- Google Maps. (2019). *Northern Territory Topological Map*, 1:50, Google Maps [online], Available at <https://www.google.com.au/maps/place/27°01'55.9%22S+131°43'52.3%22E/@-15.8849876,130.1577517,8.01z>, [accessed 19/02/2019]
- Kruskal W. H. and Wallis W. A., (1952). "Use of ranks in one-criterion variance analysis". *Journal of the American Statistical Association*. Vol. 47, No. 260, pp. 583-621
- Li, L., (1998) High-frequency over-the-horizon radar and Ionospheric backscatter studies in China, *Radio Science*, Vol. 33, pp/ 1445-1458
- Massey, F. J., (1951) "The Kolmogorov-Smirnov Test for Goodness of Fit." *Journal of the American Statistical Association*. Vol. 46, No. 253, pp. 68-78
- MATLAB Release 2018b, The MathWorks, Inc., Natick, Massachusetts, United States.
- McNamara, L. F., (1991). *The Ionosphere: Communications, Surveillance, and Direction Finding*. Malabar: Krieger Publishing Company

Munk, W. H., Nierenberg, W. A., (1969). "High frequency radar sea return and the Phillips saturation constant", *Nature*, vol. 224, p. 1285.

Neudegg, D., (2018), *Eloise Sept-15. Overview of geophysical conditions*, Ionospheric R&D Forum, PowerPoint Presentation, DST, Edinburgh

Seber, G. A. F. *Multivariate Observations*. Hoboken, NJ: John Wiley & Sons, Inc., 1984.

## Appendix A Backscatter Coefficient MATLAB Code Description

At the completion of the project, a number of MATLAB files were provided with this report. This section describes the files and how to use them to calculate the backscatter coefficient.

Note: The BSS sector numbers in all the files are enumerated from 1-8.

### A.1. RTIM and BSS Observation Temporal Matching

Script\_process\_all\_days.m calls script\_process\_bss\_im.m which temporally matches RTIM data with the available BSS sounder data. The routine grid\_save.m is called by script\_process\_bss\_im.m which saves the RTIM data. Once these ionospheric grids are saved, they can be used in the manual or automatic calculation of backscatter coefficients.

### A.2. Synthetic Backscatter Ionogram Generation

Bss\_synth\_single.m generates synthesized ionograms based on the RTIM ionospheres. A day, time index, radar and sector number needs to be selected and the code uses the ionosphere from the RTIM at that time to create a backscatter ionogram.

### A.3. Manual Data Processing and Determination of Backscatter Coefficient Values

Adjust\_day\_num.m is used to determine which days to select. Within the selected ionograms the user identifies the first-hop lobe and then identifies the region for further analysis using the routine real\_ionogram\_trim.m.

The boundary of this region is formed by drawing an upper limit and lower limit of group ranges. The user clicks (from left to right) seven times to provide an upper range limit and seven times to provide a lower range limit. These selected range extents are saved in .mat files such as freq\_cut and grp\_cut. A smooth line is generated from the clicks through interpolation to determine which cells are to be retained for further analysis.

The routine manual\_bss\_ionogram\_gen.m creates a model backscatter ionogram using PHaRLAP with the ground backscatter value set to 0 dB. Furthermore, range-frequency cells that have large contributions from F2-high and E propagation modes are flagged.

The routine real\_ionogram\_trim.m takes the values from manual\_bss\_ionogram\_gen.m and compares it to observed backscatter values. Each range-frequency cell must have passed all the filters. The backscatter values, elevation and ground ranges are all saved into a structure. This structure is saved into a file such as Backscatter\_Data\_ginput.

#### **A.4. Viewing Results from the Backscatter Coefficient Data**

The routine `data_collector.m` removes Matlab NaN values from the calculated backscatter data and places all the data into the one `.mat` file. Plots that examine the backscatter data as a function of frequency, elevation, time of day and group range are generated by `Diff_Beam_analyser.m`.

#### **A.5. Automation of Data Processing**

Attempts have been made to automate the data processing step to reduce the manual overheads. However, this process is computationally time intensive as each individual range-frequency cell is required to be checked to ensure that only 1-hop propagation modes contribute power to the cell. The ionospheres can be loaded in and backscatter values can be determined for the radar and results saved into a separate file. This automated process is not manually intensive. However, computationally there is a large burden. It may be viable to use on a large compute server.

## UNCLASSIFIED

<b>DEFENCE SCIENCE AND TECHNOLOGY GROUP DOCUMENT CONTROL DATA</b>		1. DLM/CAVEAT (OF DOCUMENT)	
2. TITLE Calculation of High Frequency Land Backscatter Coefficients		3. SECURITY CLASSIFICATION (FOR UNCLASSIFIED LIMITED RELEASE USE (U/L) NEXT TO DOCUMENT CLASSIFICATION)  Document (U) Title (U) Abstract (U)	
4. AUTHOR(S) Benjamin Slimming and Manuel Cervera		5. CORPORATE AUTHOR Defence Science and Technology Group PO Box 1500 Edinburgh SA 5111	
6a. DST GROUP NUMBER DST-Group-TR-3613	6b. AR NUMBER	6c. TYPE OF REPORT Technical Report	7. DOCUMENT DATE June 2019
8. TASK NUMBER		9. TASK SPONSOR	10. RESEARCH DIVISION National Security and Intelligence, Surveillance and Reconnaissance Division
11. MSTC High Frequency Radar		12. STC Propagation and Performance Analysis	
13. SECONDARY RELEASE STATEMENT OF THIS DOCUMENT  <i>Approved for public release</i>  OVERSEAS ENQUIRIES OUTSIDE STATED LIMITATIONS SHOULD BE REFERRED THROUGH DOCUMENT EXCHANGE, PO BOX 1500, EDINBURGH, SA 5111			
14. DELIBERATE ANNOUNCEMENT No limitations			
15. CITATION IN OTHER DOCUMENTS Yes			
16. RESEARCH LIBRARY THESAURUS High frequency radio wave backscatter, High frequency radio wave propagation, HF backscatter sounder, modelling			
17. ABSTRACT  A suitable model of the return ground clutter is required to help assess the performance of over-the-horizon radar. Currently, models for the clutter reflected from the sea exist but there are no models for the backscatter from land. The backscatter coefficient, which characterises the backscattered power, can be determined by considering the difference between observed backscatter ionograms and synthesised ionograms. The synthesised ionograms were generated using a MATLAB ray tracing toolbox, PHaRLAP, and the JORN Real Time Ionospheric Model. Data from the Laverton and Longreach backscatter sounders in September 2015 were analysed and backscatter coefficient results for sea, desert, plateau and hilly terrain in the Northern Territory were determined. It was found that the backscatter coefficient was large for hilly and rough terrains. Conversely, flat, dry deserts produced a lower backscatter coefficient.			

UNCLASSIFIED